International Journal of Hematology (2019) 110:606–617
https://doi.org/10.1007/s12185-019-02722-x

ORIGINAL ARTICLE

FF-10501 induces caspase-8-mediated apoptotic and endoplasmic reticulum stress-mediated necrotic cell death in hematological malignant cells

Taichi Matsumoto[1] · Shiro Jimi[2] · Keisuke Migita[1] · Kazuki Terada[3] · Masayoshi Mori[4] · Yasushi Takamatsu[5] · Junji Suzumiya[6] · Shuuji Hara[1]

Received: 11 March 2019 / Revised: 6 August 2019 / Accepted: 6 August 2019 / Published online: 12 August 2019

Abstract

FF-10501 is a novel inhibitor of inosine monophosphate dehydrogenase (IMPDH). Clinical trials of FF-10501 for myelodysplastic syndromes (MDS) and acute myeloid leukemia (AML) are currently being conducted in the United States. Although it has been shown that FF-10501 induces apoptosis in hematological malignant cells, the intracellular mechanisms of this effect have not been characterized. We conducted an in vitro study to elucidate the mechanisms of FF-10501-induced cell death using 12 hematological malignant cell lines derived from myeloid and lymphoid malignancies. FF-10501 suppressed the growth of each cell line in a dose-dependent manner. However, the clinically relevant dose (40 μM) of FF-10501 induced cell death in three cell lines (MOLM-13, OCI-AML3, and MOLT-3). Investigation of the cell death mechanism suggested that FF-10501 induces both apoptotic and necrotic cell death. FF-10501-induced apoptosis was mediated by caspase-8 activation followed by activation of the mitochondrial pathway in MOLM-13 and MOLT-3 cells. FF-10501 induced necrotic cell death via endoplasmic reticulum stress in OCI-AML3 cells. The present study is the first to identify intracellular pathways involved in FF-10501-induced cell death.

Keywords FF-10501 · Apoptosis · Necrosis · Caspase-8 · Endoplasmic reticulum stress

Introduction

Myelodysplastic syndromes (MDS) are a heterogeneous group of clonal disorders of hematopoietic stem and progenitor cells characterized by ineffective hematopoiesis, abnormal cell morphology, and high risk of transition to acute myeloid leukemia (AML) [1, 2]. The only potentially curative therapy for MDS is allogenic hematopoietic stem cell transplantation (HSCT). Although 30–40% of patients who undergo HSCT show long-term disease-free survival, its use is restricted to younger patients with an appropriate donor. Azacytidine is the only agent demonstrated to improve overall survival in the high-risk MDS group compared with supportive care alone [3]. However, complete remission rates in response to currently available agents are low, and recurrence is a common problem. Therefore, new therapeutic options are essential.

Inosine monophosphate dehydrogenase (IMPDH) is a rate-limiting enzyme for biosynthesis of guanine nucleotides [4]. This enzyme mediates the conversion of IMP to xanthine monophosphate, which is subjected to the

✉ Taichi Matsumoto
tmatsumoto@fukuoka-u.ac.jp

1 Department of Drug Informatics, Faculty of Pharmaceutical Sciences, Fukuoka University, 8-19-1, Nanakuma, Jounan, Fukuoka 814-0180, Japan

2 Central Laboratory of Pathology and Morphology, Department of Medicine, Fukuoka University, Fukuoka, Japan

3 Laboratory of Drug Design and Drug Delivery, Faculty of Pharmaceutical Sciences, Fukuoka University, Fukuoka, Japan

4 Department of Pharmacotherapeutics, Faculty of Pharmaceutical Sciences, Fukuoka University, Fukuoka, Japan

5 Division of Medical Oncology, Hematology, and Infectious Diseases, Department of Medicine, Fukuoka University, Fukuoka, Japan

6 Department of Oncology/Hematology, Shimane University Hospital, Shimane, Japan

synthesis of guanosine monophosphate [4]. In mammals there are two IMPDH isoforms, termed IMPDH1 and IMPDH2, which are encoded by distinct genes [5, 6]. IMPDH1 is expressed ubiquitously, while IMPDH2 has been shown to be increased in a variety of tumors including hematological malignancies [7, 8]. Therefore, targeting IMPDH is recognized as a promising therapeutic approach for hematological malignancies. FF-10501 is a novel IMPDH inhibitor and is intracellularly metabolized to mizoribine 5′-monophosphate by adenine phosphoribosyltransferase (APRT), which inhibits IMPDH [9]. Currently, a clinical trial for FF-10501 in patients with relapsed or refractory hematological malignancies, including MDS and AML, is being conducted in the United States, and FF-10501 treatment has resulted in partial remissions and stabilized disease status without severe side effects (https://clinicaltrials.gov/ct2/show/NCT02193958, https://clinicaltrials.gov/ct2/show/NCT03194685). Previous studies have detailed the anti-tumor characteristics of FF-10501 in vitro. Murase et al. [10] showed that FF-10501 effectively killed cells resistant to azacytidine, decitabine, and cytarabine, suggesting that FF-10501 could be an alternative treatment to azacytidine in patients with leukemia. Ichii et al. [11] demonstrated that FF-10501 promoted differentiation to erythroid and myeloid lineages via production of reactive oxygen species followed by the activation of the mitogen-activated protein kinase pathway. Moreover, Yang et al. [12] demonstrated the induction of apoptosis in myeloid leukemia cells by FF-10501. However, the intracellular mechanisms of FF-10501-induced cell death have not been characterized.

We conducted this study to elucidate the mechanisms of action of FF-10501 in hematological malignant cultured cell lines and found that FF-10501 induced not only apoptotic but also necrotic cell death. FF-10501-induced apoptotic cell death was induced by activation of caspase-8 and mitochondrial pathway. FF-10501-induced necrotic cell death was mediated by endoplasmic reticulum (ER) stress. For the first time, we characterized the mechanisms of action of cell death induced by FF-10501.

Materials and methods

Cell culture

We used 12 cell lines derived from a variety of hematological malignant diseases: two cell lines established from patients with AML at relapse after initial MDS (MOLM-13, SKM-1), two acute promyelocytic leukemia cell lines (HL-60, NB-4), two de novo AML cell lines (OCI-AML3, THP-1), two CML cell lines (K562, MEG-01), two acute T lymphoblastic leukemia cell lines (MOLT-3, Jurkat), Burkitt's lymphoma cell line (Raji), and a multiple myeloma cell line (RPMI8226). NB-4, THP-1, K562, MEG-01, MOLT-3, Jurkat, Raji, and RPMI8226 cells were purchased from ATCC (VA, USA). HL-60 cells were from RIKEN Inc. (Tokyo, Japan). OCI-AML3 cells were from DSMZ (Braunschweig, Germany). MOLM-13 and SKM-1 cells were kindly provided by FUJIFILM Corporation. All cell lines were maintained in RPMI1640 with 10% fetal bovine serum (ThermoFisher Scientific, MA, USA) and 1% penicillin and streptomycin (FUJIFILM Wako Pure Chemical Corporation, Osaka, Japan). The cells were cultured at 37 °C in a humidified atmosphere of 5% CO_2 in air.

Measurement of cell viability

Cell viability was measured using PrestoBlue Viability Reagent (ThermoFisher Scientific, MA, USA) according to the manufacturer's instructions. Fluorescence intensity was measured using a DTX 880 Multimode Detector (Beckman Coulter Inc. CA, USA). Curves were generated and GI_{50} was calculated using Prism 6 (GraphPad Software, CA, USA).

Measurement of the percentage of viable cells

Cells were stained with GUAVA ViaCount Reagent (Merck KGaA, Darmstadt, Germany) according to the manufacturer's instructions, and fluorescence intensity was analyzed using GUAVA ViaCount software in GUAVA PCA (Merck KGaA, Darmstadt, Germany).

Annexin V/PI staining

Cells were stained using MEBCYTO® Apoptosis Kit (Annexin V-FITC Kit) (Medical and Biological Laboratories Co., Ltd, Nagoya, Japan) according to the manufacturer's instructions. Fluorescence was detected using FACSVerse (BD Biosciences, NJ, USA).

Analysis of mitochondrial membrane potential ($\Delta\psi_m$)

Cells were stained using 100 nM of MitoTracker Orange CMTMRos (ThermoFisher Scientific, MA, USA) according to the manufacturer's instructions. Fluorescence was detected using FACSVerse (BD Biosciences, NJ, USA).

Flow cytometric TUNEL assay

Cells were fixed in 1% paraformaldehyde for 15 min on ice and then permeabilized in ice-cold 70% ethanol at − 20 °C overnight. The cells were then stained using a

GUAVA TUNEL Kit (Merck KGaA, Darmstadt, Germany) according to the manufacturer's instructions. Fluorescence was measured using FACSVerse (BD Biosciences, NJ, USA).

Western blotting

Cells were lysed in 2% SDS lysis buffer (Tris-buffered saline containing 2% SDS and protease inhibitor cocktail), then sonicated. Nuclear fractions were extracted using EzSubcell Extract (ATTO, Tokyo, Japan) according to the manufacturer's instructions. Protein concentrations of cell lysates were determined using the Pierce™ BCA Protein Assay Kit (ThermoFisher Scientific, MA, USA). Cell lysates containing 10 μg of protein were fractionated by SDS-PAGE on a 4–15% mini-protean TGX precast gel (Bio-Rad, CA, USA), then transferred to Immun-blot PVDF membranes (Bio-Rad, CA, USA). Membranes were blocked with 5% bovine serum albumin (BSA) containing Tris-buffered saline with 0.1% Tween 20 (TBST) for 1 h at room temperature. Membranes were then incubated with primary antibodies. Antibodies were purchased from Cell Signaling Technology, Inc., except for anti-caspase-8 antibody, anti-cytochrome c antibody, and anti-BID antibody, which was purchased from Santa Cruz Biotechnology, BioLegend, and R&D Systems respectively. The following antibodies were incubated as follows: anti-Bax (Cat#: 2772), anti-Mcl-1 (Cat#: 4572), anti-cytochrome c (Cat#: 612301), anti-caspase-9 (Cat#: 9502), anti-caspase-8 (Cat#: sc-56070), anti-cleaved caspase-8 (Cat#: 9496), anti-caspase-3 (Cat#: 9662), anti-poly(ADP-ribose) polymerase (PARP) (Cat#: 9542), anti-cleaved PARP (Cat#: 5625), anti-β-actin (Cat#: 4970), anti-BID (Cat#: AF860-SP), anti-apoptosis inducing factor (AIF) (Cat#: 5318), anti-endonuclease G (Endo G) (Cat#: 4969), anti-Histone H3 (Cat#: 9717), and anti- CCAAT/enhancer-binding protein homologous protein (CHOP) (Cat#: 2895) antibodies were incubated in 5% BSA containing TBST overnight at 4 °C. Membranes were washed three times and incubated with horseradish peroxidase-linked anti-rabbit IgG (Cat#: 7074) or anti-mouse IgG (Cat#: 7076) in 5% BSA containing TBST for 1 h at room temperature. After the membranes were washed three times with TBST, immunostaining was visualized with 20× LumiGLO® Reagent and 20× Peroxide (Cell Signaling Technology, Inc.) using a ChemiDoc Touch imaging system (Bio-Rad).

Statistical analysis

Values are expressed as mean ± standard deviation. Statistical comparisons were made using one-way ANOVA. $P < 0.05$ was considered statistically significant.

Results

Growth inhibitory and cytotoxic effects of FF-10501 on hematological malignant cells

To investigate the anti-tumor effects of FF-10501 on hematological malignant cells, 12 human hematological malignant cell lines were treated with 0–1000 μM FF-10501 for 72 h. Cell viability was measured and the concentration of FF-10501 that inhibited the growth of cells by 50% (GI_{50}) was calculated. FF-10501 reduced cell viability of each cell line, but the response to FF-10501 varied between the cell types (Fig. 1a; Table 1). We defined high sensitivity as GI_{50} less than 40 μM and low sensitivity as GI_{50} greater than 40 μM because previous reports demonstrated that the maximum plasma concentration following oral administration of FF-10501 was ~ 56 μM [11]. Among the eight myeloid cell lines, six cell lines (MOLM-13, SKM-1, NB-4, OCI-AML3, THP-1, and K562) showed high sensitivity to FF-10501. Both acute T lymphoblastic leukemia (T-ALL) cell lines (MOLT-3 and Jurkat) also showed excellent response to FF-10501. In contrast, B cell lineage cell lines (Raji and RPMI8226) showed low sensitivity to FF-10501.

To investigate whether FF-10501 induced cell death in FF-10501-sensitive cell lines, we measured the percentage of viable cells following treatment with 0 or 40 μM FF-10501 for 72 h. FF-10501 strongly induced cell death in MOLM-13, OCI-AML3, and MOLT-3 cells. In contrast, FF-10501 was only slightly cytotoxic toward the other cell lines evaluated (Fig. 1b). These results showed that a clinical dose of FF-10501 exerted anti-proliferative effects on SKM-1, HL-60, NB-4, THP-1, K562, MEG-01, Jurkat, Raji, and RPMI8226 cells and cytotoxic effects on MOLM-13, OCI-AML3, and MOLT-3 cells.

Type of cell death by FF-10501

To investigate the type of cell death induced by FF-10501, MOLM-13, OCI-AML3, and MOLT-3 cells were treated with 0 or 40 μM FF-10501 for 72 h, then stained with annexin V/PI to distinguish between apoptotic and necrotic cells as below; apoptotic cells: annexin V^+PI^-, necrotic cells: annexin V^+PI^+ [13]. Treatment with FF-10501 increased annexin V^+PI^- cells and annexin V^+PI^+ cells in MOLM-13 and MOLT-3 cells, whereas it largely increased annexin V^+PI^+ cells with slight increase of annexin V^+PI^- cells in OCI-AML3 cells (Fig. 2a). We also performed TUNEL assay to evaluate fragmentation of genomic DNA associated with apoptosis. TUNEL positive cells were 14.9%, 16.7%, and 25.8% in MOLM-13,

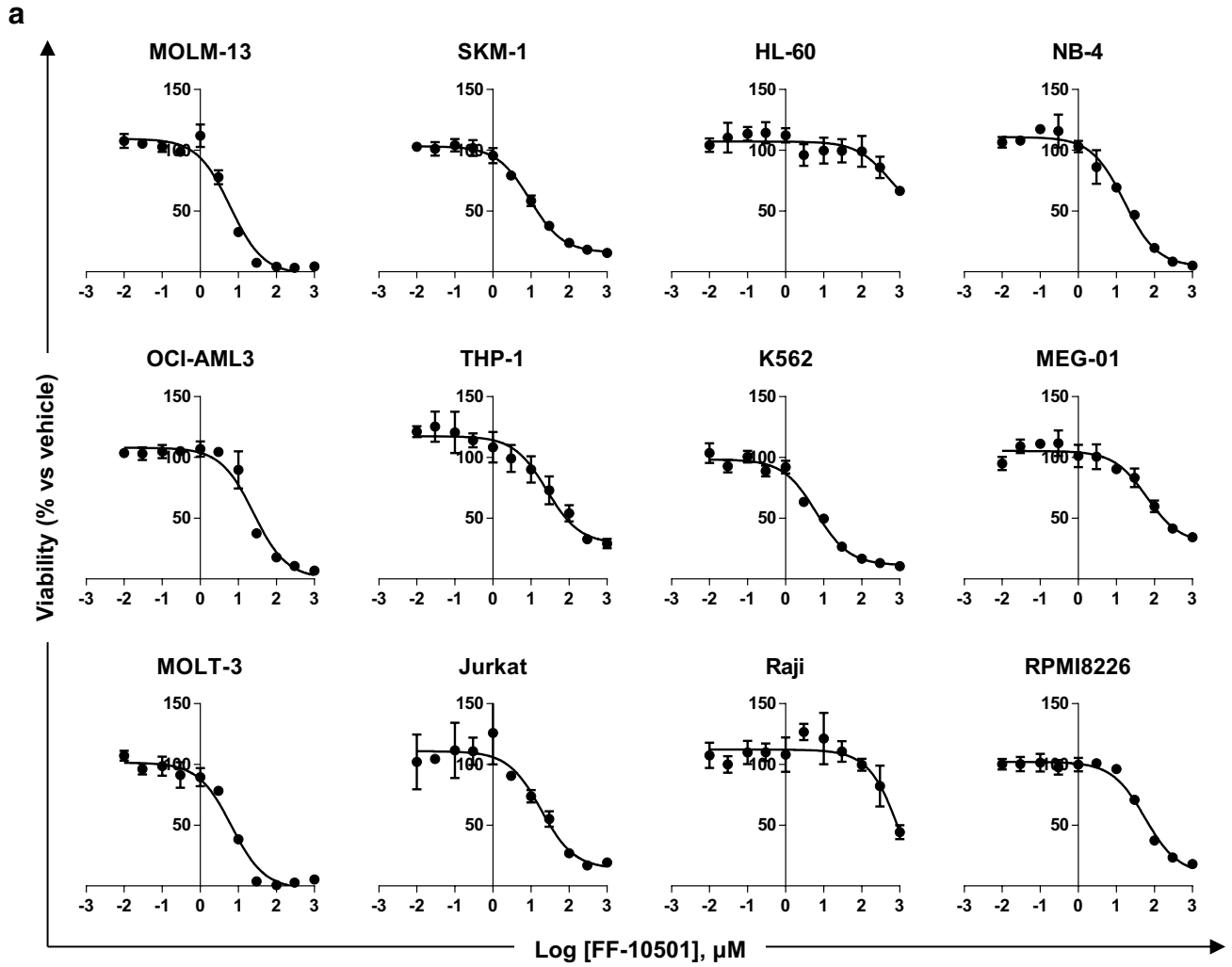
a
MOLM-13
SKM-1
HL-60
NB-4
OCI-AML3
THP-1
K562
MEG-01
MOLT-3
Jurkat
Raji
RPMI8226
Viability (% vs vehicle)
Log [FF-10501], μM

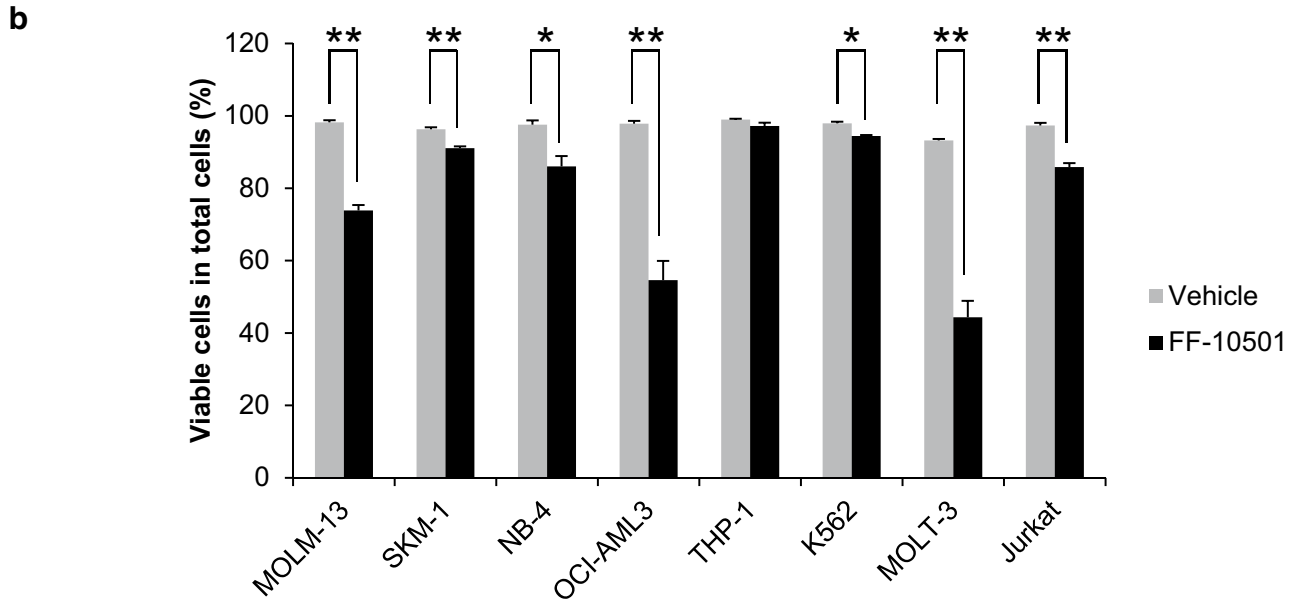
b
Viable cells in total cells (%)
MOLM-13
SKM-1
NB-4
OCI-AML3
THP-1
K562
MOLT-3
Jurkat
Vehicle
FF-10501

◂**Fig. 1** Anti-tumor effects of FF-10501 in hematological malignant cells. **a** Cell viability of the indicated cell lines treated with 0.01–1000 μM of FF-10501 for 72 h. **b** The percentage of viable cells of the indicated cell lines treated with vehicle or 40 μM FF-10501 for 72 h. Experiments were repeated in triplicate and results are reported as the mean ± SD of these replicates. $^{**}P < 0.01$, $^{*}P < 0.05$

Table 1 GI_{50} of FF-10501 in hematological malignant cells

Cell line	GI_{50} (μM)	
	Mean ± SE	95% CI
MOLM-13	6.1 ± 1.2	4.6–8.0
SKM-1	9.3 ± 1.1	7.6–11.3
HL-60	530.9 ± 2.2	97.5
NB-4	16.2 ± 1.2	11.7–22.3
OCI-AML3	25.1 ± 1.2	18.4–34.2
THP-1	25.8 ± 1.3	13.8–47.2
K562	6.3 ± 1.1	4.7–8.5
MEG-01	63.1 ± 1.3	37.7–105.0
MOLT-3	6.6 ± 1.2	4.9–8.8
Jurkat	18.5 ± 1.4	9.8–34.8
Raji	1297.2 ± 2.6	325.1
RPMI8226	56.6 ± 1.1	44.0–73.1

OCI-AML3, and MOLT-3 cells, respectively. (Figure 2b). The percentage of TUNEL positive cells was smaller than percentage of total annexin V positive cells and comparable with percentage of annexin V^+PI^- positive cells (Fig. 2a, b). These results indicated that FF-10501 induced apoptotic and necrotic cell death in MOLM-13 and MOLT-3 cells, whereas it mainly induced necrotic cell death in OCI-AML3 cells.

Effect of FF-10501 on mitochondrial membrane potential

We next investigated induction of intracellular apoptosis pathways by FF-10501. Since loss of mitochondrial membrane potential ($\Delta\psi_m$) is involved in the induction of apoptosis, we determined $\Delta\psi_m$ in MOLM-13, OCI-AML3, and MOLT-3 cells treated with 0 or 40 μM FF-10501 for 24 h (Fig. 3a). We observed loss of $\Delta\psi_m$ in 24.3% and 24.4% of MOLM-13 and MOLT-3 cells, respectively. In contrast, the decrease in Δψm was significant but small in OCI-AML3 cells. Bcl-2 family proteins are associated with retention of $\Delta\psi_m$ and the dysregulation of expression of Bcl-2 family proteins cause disruption of $\Delta\psi_m$ followed by apoptosis [14]. Therefore, we examined the effect of FF-10501 on expression of Bcl-2 family proteins, such as Bax and Mcl-1. FF-10501 increased Bax expression in MOLT-3 cells but not in MOLM-13 and OCI-AML3 cells. Mcl-1 expression was decreased by FF-10501 in MOLM-13 and MOLT-3 but not in OCI-AML3 cells (Fig. 3b). FF-10501 increased cytosolic cytochrome c in MOLM-13 and MOLT-3 but not in OCI-AML3 cells (Fig. 3c). These results suggested that the mitochondria-mediated pathway was associated with FF-10501-induced apoptosis in MOLM-13 and MOLT-3 cells, whereas the contribution of mitochondria was only marginal in FF-10501-induced cell death in OCI-AML3 cells.

Caspase-8 activation by FF-10501

Caspase cleavage is associated with induction of apoptosis [15]. Caspase-9 and -8 are initiators of and caspase-3 executes apoptosis [15]. Therefore, we performed western blotting to analyze the expression of full-length and cleaved forms of caspase-9, -8 and -3 in MOLM-13, OCI-AML3, and MOLT-3 cells treated with 0 or 40 μM FF-10501 for 24 h (Fig. 4a). The expression of cleaved caspase-9 did not change in response to FF-10501 in MOLM-13 and OCI-AML3 cells, and slightly increased in MOLT-3 cells. In contrast, cleaved caspase-8 level was greatly increased in MOLM-13 and MOLT-3 cells, but not in OCI-AML3 cells, in response to FF-10501. Similar results were observed for the cleaved form of caspase-3 and poly(ADP-ribose) polymerase (PARP), which are downstream effectors of caspase-8. Caspase-8 activates BH3 interacting-domain death agonist (BID) and truncated BID (tBID) promotes permeabilization of mitochondrial membrane [16]. Western blotting analysis showed that FF-10501 reduced cytosolic BID in MOLM-13 and MOLT-3 cells but not in OCI-AML3 cells (Fig. 4b). These results suggested that the caspase-8/BID/mitochondria pathway was associated with apoptosis induction in MOLM-13 and MOLT-3 cells. Accumulation of apoptosis-inducing factor (AIF) and endonuclease G (Endo G) in the nucleus is a hallmark of caspase-independent apoptosis. We examined whether FF-10501 promoted accumulation of AIF and Endo G in the nucleus of OCI-AML3 cells. Nuclear fractions of MOLM-13, OCI-AML3, and MOLT-3 treated with 0 or 40 μM FF-10501 for 24 h were subjected to western blot analysis for AIF and Endo G (Fig. 4c). AIF expression was increased by treatment with FF-10501 in MOLM-13 and MOLT-3 cells, but not in OCI-AML3 cells, while FF-10501 did not change the expression of Endo G in any of the three cell lines. These results indicated that FF-10501 induced apoptosis in MOLM-13 and MOLT-3 cells via caspase-dependent and caspase-independent pathways, and that OCI-AML3 cells were killed by FF-10501 via other mechanisms.

We further examined the effect of pan-caspase inhibitor Z-VAD-FMK on cell death induced by FF-10501. Z-VAD-FMK attenuated activation of caspase-8 and -3 in MOLM-13 and MOLT-3 cells (Fig. 5a). In this condition, Z-VAD-FMK did not show any effect on cytotoxicity of FF-10501

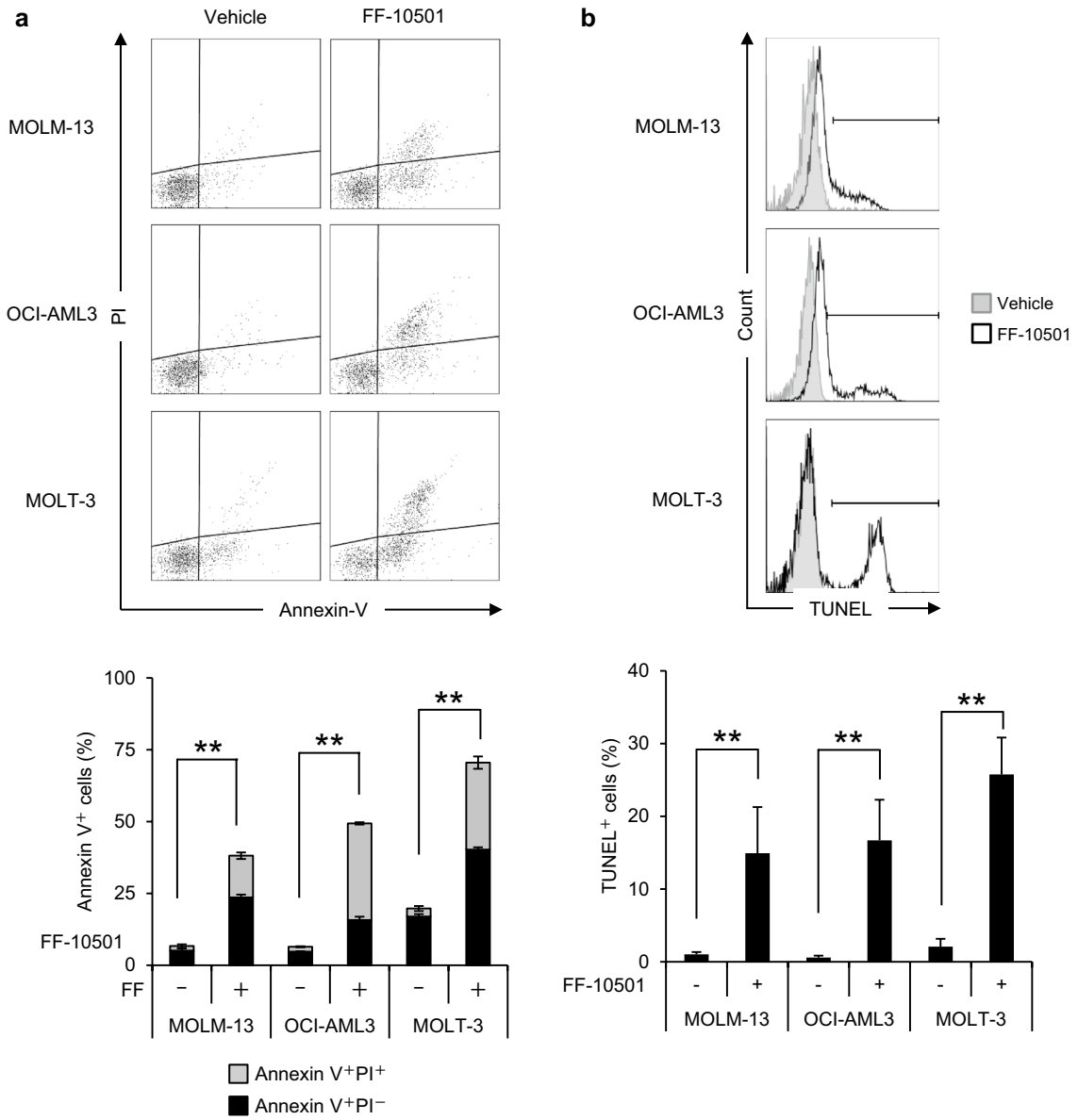

Fig. 2 Induction of apoptosis and necrosis by FF-10501. **a** Dot plot of annexin V/PI staining and **b** TUNEL staining of MOLM-13, OCI-AML3, and MOLT-3 cells treated with vehicle or 40 μM of FF-10501 for 72 h. Experiments repeated in triplicate and results are expressed as the mean ± SD of these replicates. $^{**}P < 0.01$

in MOLM-13 and MOLT-3 cells (Fig. 5b). Interestingly, Z-VAD-FMK decreased annexin V^+PI^- cells and increased annexin V^+PI^+ cells with no change in total annexin V^+ cells in MOLM-13 and MOLT-3 cells (Fig. 5c), indicating that Z-VAD-FMK switched cell death type from apoptosis to necrotic cell death. These results suggested that caspases, especially caspase-8, were involved in the regulation of cell death type in MOLM-13 and MOLT-3 cells. Cell death and annexin V positivity in OCI-AML3 cells were not affected by Z-VAD-FMK (Fig. 5b, c), indicating that FF-10501-induced cell death in OCI-AML3 cells were independent of caspase activation.

Involvement of ER stress in FF-10501-induced necrosis

Since receptor-interacting protein (RIP1) is a central mediator of necrotic cell death [17], we examined the effect of necrostatin-1 (Nec-1), a RIP1 inhibitor, on FF-10501-induced cell death in OCI-AML3 cells. Nec-1 did not affect FF-10501-induced cell death in OCI-AML3 cells (Fig. 6a). Previous reports showed that ER stress induces apoptosis and necrosis independent of caspase activation [18]. Therefore, we examined whether ER stress was associated with FF-10501-induced necrosis in OCI-AML3 cells. OCI-AML3

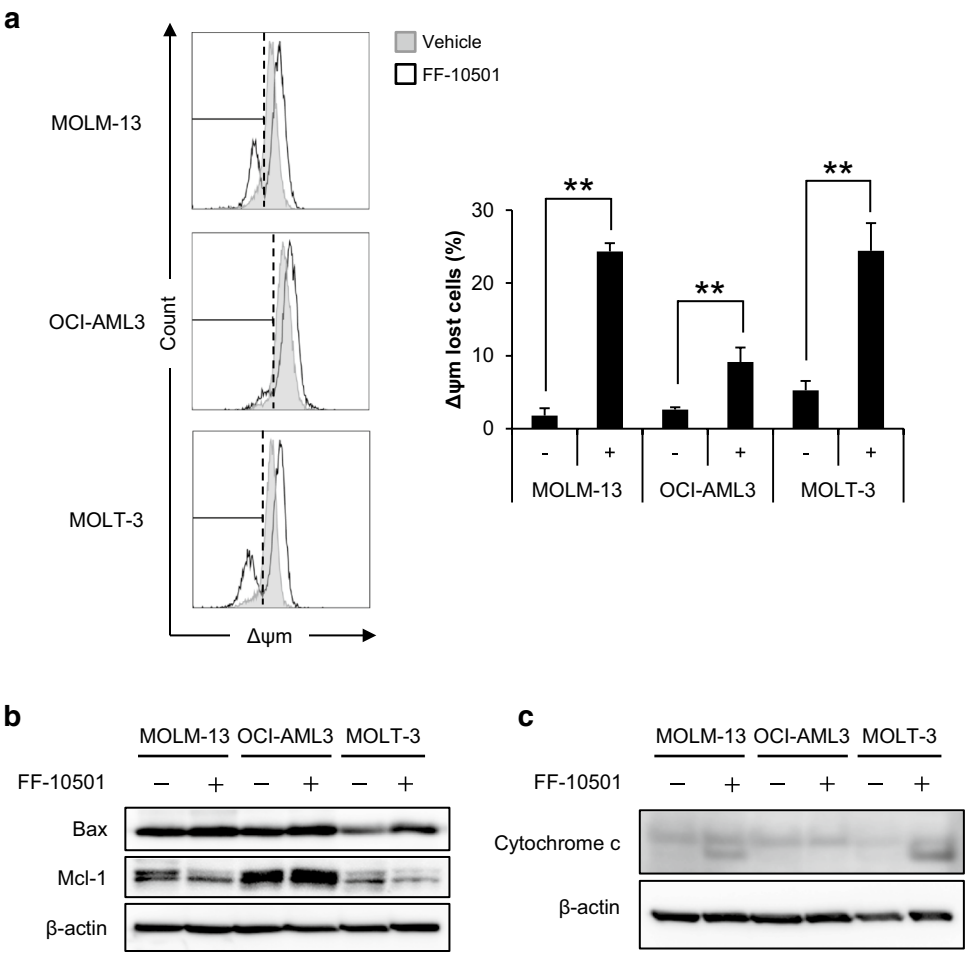

Fig. 3 Effect of FF-10501 on the mitochondria-mediated apoptosis pathway. **a** Histogram of Δψm in MOLM-13, OCI-AML3, and MOLT-3 cells treated with vehicle (gray filled histogram) or 40 μM of FF-10501 (black line) for 72 h. Experiments were repeated in triplicate and results are expressed as the mean ± SD of these replicates. $^{**}P < 0.01$. **b**, **c** The expression of Bax and Mcl-1 (**b**) and cytochrome c (**c**) in the cytoplasm of MOLM-13, OCI-AML3, and MOLT-3 cells treated with 0 or 40 μM of FF-10501 for 24 h

cells were treated with FF-10501 in the absence or presence of 4-phenyl butyric acid (4-PBA), a chemical chaperone used to suppress ER stress, and the percentage of viable cells was measured. 4-PBA abrogated FF-10501-induced cytotoxicity in OCI-AML3 cells in a dose-dependent manner (Fig. 6b). Moreover, annexin V/PI staining showed that the FF-10501-induced increase in annexin V^+PI^+ cells was blocked by 4-PBA in a dose-dependent manner, while the increase of annexin V^+PI^- cells by FF-10501 was not affected by 4-PBA (Fig. 6c). FF-10501 induced the expression of C/EBP homologous protein (CHOP), a crucial mediator of ER stress-induced cell death (Fig. 6d), and 4-PBA suppressed FF-10501-induced CHOP expression in OCI-AML3 cells (Fig. 6e). These results suggested that ER stress was associated with FF-10501-induced necrosis in OCI-AML3 cells.

Discussion

In this study, we demonstrated that FF-10501 induced apoptosis and necrosis in hematological malignant cells via at least two different signaling mechanisms in a cell type-dependent manner: caspase-8-mediated apoptosis and ER stress-mediated necrosis. Previous studies demonstrated the anti-tumor effects of FF-10501 on hematological malignant cells. Yang et al. [12] showed that a clinically relevant dose (~40 μM) of FF-10501 suppressed the proliferation of 10 myeloid leukemia cell lines and induced apoptosis in three cell lines. Ichii et al. [11] reported that FF-10501 promoted erythroid differentiation in hematological malignant cells and $CD34^+$ hematopoietic progenitor cells. However, the intracellular mechanisms of FF-10501-induced cell death have not been characterized. The present study was the first to show the cell death pathways induced by FF-10501.

We first determined the anti-tumor properties of FF-10501 using cell lines derived from a variety of hematological malignant cell lines including myeloid and lymphoid cell lines. Consistent with previous studies [10–12], FF-10501 suppressed cell growth of all cell lines evaluated in this study, but the sensitivity varied (Fig. 1, Table 1). FF-10501 substantially inhibited growth of myeloid leukemia cells, except for HL-60 and MEG-01 cells. Previous studies showed that IMPDH is over-expressed in myeloid leukemia cells, and the IMPDH inhibitor tiazofurin exerted

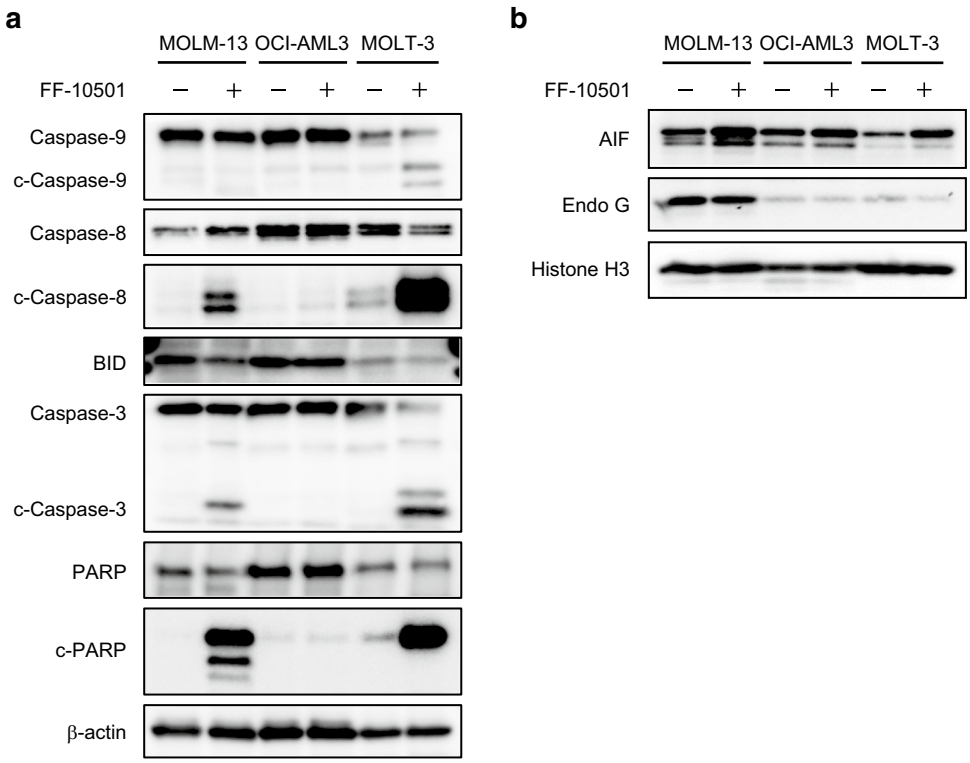

Fig. 4 The effect of FF-10501 on caspase activity. **a** The expression of caspase-9, caspase-8, BID, caspase-3, and PARP in MOLM-13, OCI-AML3, and MOLT-3 cells treated with vehicle or 40 μM FF-10501 for 24 h. β-actin was used as a reference protein for whole cell lysates. **b** The expression of AIF and Endo G in the nuclear fractions of MOLM-13, OCI-AML3 and MOLT-3 cells treated with vehicle or 40 μM FF-10501 for 24 h. Histone H3 was used as a reference protein for the nuclear fraction. GAPDH, a major marker for the cytoplasmic fraction, was not detected in this fraction (data not shown)

anti-leukemia activity in a phase II study [19]. In addition, a recent report showed that IMPDH is the rate-limiting enzyme for synthesis of guanine nucleotides and is a transcription factor for oncogenes including *Myc*, which is associated with transformation and progression of cancer cells [20]. An IMPDH inhibitor, ribavirin, suppressed *Myc* gene expression [21]. Therefore, IMPDH inhibitors, including FF-10501, could be effective drugs to suppress growth of myeloid leukemia cells and to abrogate transformation of MDS to AML and inhibit CML blast crisis. Interestingly, FF-10501 also strongly suppressed growth of T-ALL cell lines in our study (Fig. 1a). A recent report showed that IMPDH inhibition is a promising approach for a part of T cell acute lymphoblastic leukemia (T-ALL). For example, Tzoneva et al. [22] showed that a gain-of-function mutation of the 5′-nucleotidase cytosolic II (NT5C2), which is involved in resistance to 6-mercaptopurine and relapse of pediatric T-ALL, and inhibition of IMPDH using mizoribine, induced cytotoxicity against NT5C2-mutant leukemia lymphoblasts. FF-10501 may also be effective in T-ALL with mutation of NT5C2. In contrast, B-cell lineage malignant cells tend to be resistant to FF-10501 (Fig. 1a). Ishituka et al. [23] reported that an IMPDH inhibitor, VX-944, induced apoptosis in multiple myeloma cell lines. Further studies should investigate the cell type-dependent regulatory factor involved in FF-10501 activity. In addition, further investigations should examine the correlation between GI_{50} and the expression of APRT, IMPDH, and hypoxanthine–guanine phosphoribosyltransferase (a rate-limiting enzyme in the salvage pathway of purine nucleotide synthesis).

FF-10501 was thought to induce intrinsic apoptosis via caspase-8/BID/mitochondria cascade in MOLM-13 and MOLT-3 cells (Figs. 3, 4). In these cells, the pan-caspase inhibitor Z-VAD-FMK did not suppress FF-10501-induced cell death and switched the mode of cell death (Fig. 5). Z-VAD-FMK has been shown to block apoptosis and sensitized to necrotic and autophagic cell death [24]. RIP1 plays a central role in induction of necrotic cell death [17]. Stimulation of death receptor results in activation of both caspase-8. The RIP1 transduces apoptotic and necrotic signaling while activated caspase-8 inactivates RIP1 by proteolysis followed by inhibition of necrotic signaling [25]. Thus, inhibition of caspase-8 by Z-VAD-FMK inhibits apoptosis and sensitizes to necrotic cell death [26]. Therefore, the switching of FF-10501-induced cell death by Z-VAD-FMK could explain the involvement of caspase-8 in FF-10501-induced apoptosis in MOLM-13 and MOLT-3 cells.

Caspase-8 is well characterized as an essential mediator of extrinsic apoptotic pathway through the stimulation of death receptors [27]. We cannot exclude the possibility that FF-10501 may have induced the secretion of ligands for death receptors. Notably, previous studies demonstrated the suppressive effect of IMPDH inhibitors on cytokine secretion by hematopoietic cells [28, 29]. On the other hand, it

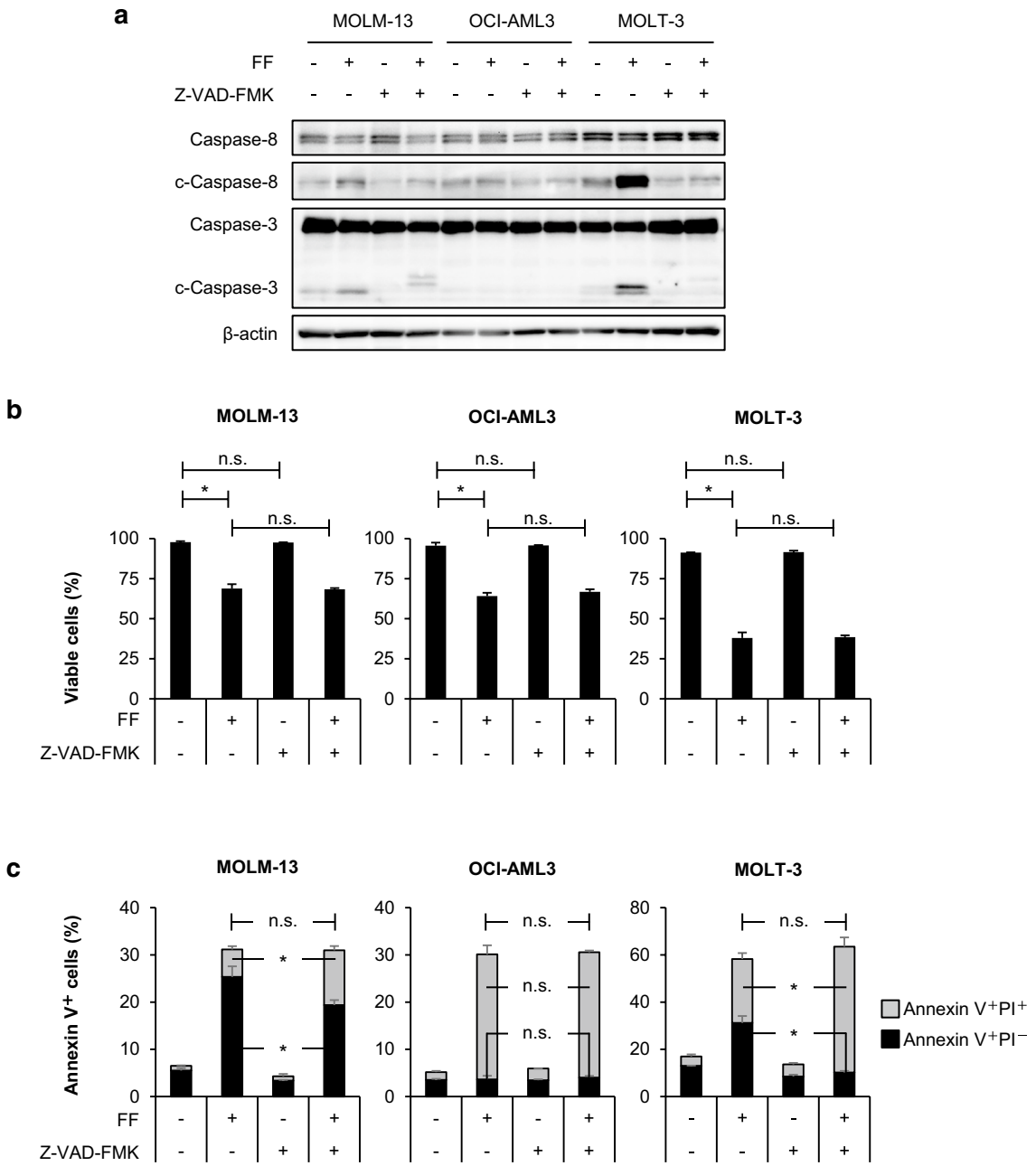

Fig. 5 The effect of caspase inhibition on FF-10501-induced cell death. **a** The expression of full-length and cleaved form of caspase-8 and -3 in MOLM-13, OCI-AML3 and MOLT-3 cells treated with vehicle or 40 μM FF-10501 in absence or presence of Z-VAD-FMK for 24 h. β-actin was used as a reference protein for whole cell lysates. **b**, **c** Percentage of viable cells (**b**) and annexin V^+ cells (**c**) in OCI-AML3 cells treated with 0 or 40 μM FF-10501 in absence or presence of Z-VAD-FMK for 48 h. Experiments were repeated in triplicate, and results are expressed as the mean ± SD of these replicates. $^*P < 0.05$

has been shown that caspase-8 is activated independently of death receptor. Several anti-cancer drugs (e.g. etoposide and mitomycin c) activated caspase-8 in CD95-deficient cells [30]. Sphingosine has been reported to induce apoptosis via caspase-8 activation in Fas-associated death domain (FADD)-deficient cells [31]. Although the precise mechanisms are still unknown, FF-10501 may induce intrinsic apoptosis via activation of caspase-8 independently of death receptor.

Interestingly, characteristics of FF-10501-induced cell death in OCI-AML3 were totally different from MOLM-13 and MOLT-3 cells. As FF-10501-treated OCI-AML3 cells were almost annexin V^+PI^+ cells, FF-10501 was thought to induce necrosis in OCI-AML3 cells. FF-10501-induced

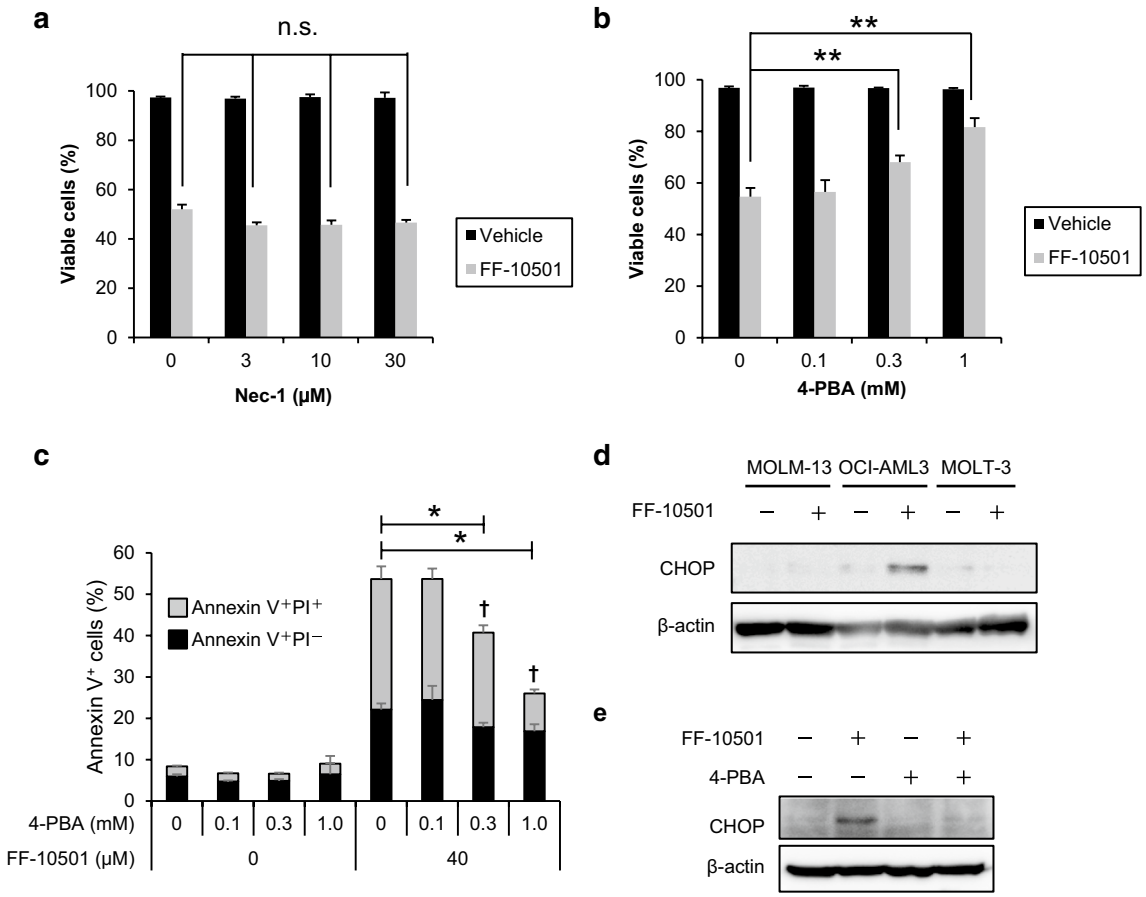

Fig. 6 Involvement of ER stress in FF-10501-induced apoptosis in OCI-AML3 cells. **a** Percentage of viable cells in OCI-AML3 cells treated with 0 or 40 μM FF-10501 in the absence or presence of various concentrations of Nec-1 (**a**) and 4-PBA (**b**) for 48 h. $^{**}P<0.01$. **c** Percentage of annexin V^+ OCI-AML3 cells treated with 40 μM FF-10501 in the absence or presence of various concentrations of 4-PBA for 72 h. $^{*}P<0.05$ for total annexin V^+ cells vs. treatment with FF-10501 alone, $^{\dagger}P<0.05$ for annexin V^+PI^+ cells vs. treatment with FF-10501 alone. Experiments were repeated in triplicate and results are expressed as the mean ± SD of these replicates. **d** The expression of CHOP in MOLM-13, OCI-AML3 and MOLT-3 cells treated with vehicle or 40 μM FF-10501 for 24 h. **e** The expression of CHOP in OCI-AML3 cells treated with vehicle or 40 μM FF-10501 in absence or presence of 1 mM 4-PBA for 24 h

cell death in OCI-AML3 was affected by neither Z-VAD-FMK nor Nec-1 (Figs. 5b, 6a). Chaigne-Delalande et al. [32] reported that IMPDH inhibitor mycophenolic acid induced necrosis defined by loss of plasma membrane integrity, mitochondria swelling, and no trace of chromatin condensation, and MPA-induced necrosis was not abrogated by either Z-VAD-FMK or knockout of RIP1. This report is well in line with our current study and supports the induction of necrotic cell death by IMPDH inhibitor including FF-10501. OCI-AML3 cells are AML cell lines with mutant nucleophosmin (NPM1), which is observed in 35% of patients with AML [33]. A previous study reported that mutant NPM1 inhibited caspase-8 through direct interaction with cleaved form of caspase-8 [34]. It is possible that the inhibition of casapase-8 by mutant NPM1 blocked apoptotic signaling instead of induction of necrotic signaling by FF-10501 in OCI-AML3 cells. Impairment and evasion of apoptosis are hallmarks of various cancers, including hematological malignancies, that contribute to tumor initiation, progression and treatment resistance [35]. Resistance to chemotherapy is currently a major problem in cancer treatment, and it is frequently associated with failure of tumor cells to undergo apoptosis [35, 36]. Therefore, there is an urgent need to develop new therapies to promote cell death in cancers. Inducers of necrotic cell death, for example FF-10501, may offer an alternative option to trigger apoptosis-resistant cancer cell death.

How FF-10501 activates caspase-8 was unknown until now. We observed that FF-10501 induced the loss of $\Delta\psi_m$ while a large population of cells seemed to be increased the fluorescence of $\Delta\psi_m$ indicator. We used MitoTracker Orange CMTMRos to measure $\Delta\psi_m$ in this study. According to manufacturer's instruction, this dye specifically accumulates in active mitochondria and is oxidized by reactive oxygen species (ROS) produced in

electron transfer system of the mitochondria, thus resulting in the generation of fluorescence. Therefore, the increase in MitoTracker's fluorescence in FF-10501-treated cells, as observed in our study, was suspected to have resulted from ROS production by FF-10501. Consistent with this, in a previous study, FF-10501 was reported to induce cell differentiation via ROS production [10]. Further investigations are needed to elucidate how FF-10501 activates caspase-8.

In summary, we demonstrated that FF-10501 induces apoptotic and necrotic cell death in hematological malignant cells, including myeloid cells and lymphoid cells, via caspase-8 activation or ER stress in a cell type-dependent manner. The current study provides mechanistic evidence of anti-tumor characteristics of FF-10501, a promising therapeutic drug for the treatment of hematological malignancies, including MDS and AML.

Acknowledgements The authors would like to thank Miyuki Saisho, Eri Sakai-Nagamatsu, Misato Yagi, Mami Sato, Miku Kamekou, Ayaka Tsuzuki, Takafumi Kuroiwa, Midori Suekane, Kousuke Iwasaki, and Shuntarou Nakamura for their help with the experiments.

Author contributions TM and SJ designed the research study. TM performed the experiments. TM, SJ, KT, and MM analyzed and interpreted the data. TM drafted the manuscript. SJ, KM, YT, JS, and SH revised the manuscript. SJ provided final approval of the current version for submission.

Funding This research was partially supported by FUJIFILM Corporation.

Compliance with ethical standards

Conflict of interest The authors declare that they have no conflict of interest.

References

1. Cazzola M, Della Porta MG, Malcovati L. The genetic basis of myelodysplasia and its clinical relevance. Blood. 2013;122(25):4021–34. https://doi.org/10.1182/blood-2013-09-381665.
2. Yoshimi A, Abdel-Wahab O. Splicing factor mutations in MDS RARS and MDS/MPN-RS-T. Int J Hematol. 2017;105(6):720–31. https://doi.org/10.1007/s12185-017-2242-0.
3. Fenaux P, Mufti GJ, Hellstrom-Lindberg E, Santini V, Finelli C, Giagounidis A, et al. Efficacy of azacitidine compared with that of conventional care regimens in the treatment of higher-risk myelodysplastic syndromes: a randomised, open-label, phase III study. Lancet Oncol. 2009;10(3):223–32. https://doi.org/10.1016/S1470-2045(09)70003-8.
4. Hedstrom L. IMP dehydrogenase: structure, mechanism, and inhibition. Chem Rev. 2009;109(7):2903–28. https://doi.org/10.1021/cr900021w.
5. Collart FR, Huberman E. Cloning and sequence analysis of the human and Chinese hamster inosine-5′-monophosphate dehydrogenase cDNAs. J Biol Chem. 1988;263(30):15769–72.
6. Natsumeda Y, Ohno S, Kawasaki H, Konno Y, Weber G, Suzuki K. Two distinct cDNAs for human IMP dehydrogenase. J Biol Chem. 1990;265(9):5292–5.
7. Jackson RC, Weber G, Morris HP. IMP dehydrogenase, an enzyme linked with proliferation and malignancy. Nature. 1975;256(5515):331–3.
8. Senda M, Natsumeda Y. Tissue-differential expression of two distinct genes for human IMP dehydrogenase (E.C.1.1.1.205). Life Sci. 1994;54(24):1917–26.
9. Fukui M, Inaba M, Tsukagoshi S, Sakurai Y. New antitumor imidazole derivative, 5-carbamoyl-1H-imidazol-4-yl piperonylate, as an inhibitor of purine synthesis and its activation by adenine phosphoribosyltransferase. Cancer Res. 1982;42(3):1098–102.
10. Murase M, Iwamura H, Komatsu K, Saito M, Maekawa T, Nakamura T, et al. Lack of cross-resistance to FF-10501, an inhibitor of inosine-5′-monophosphate dehydrogenase, in azacitidine-resistant cell lines selected from SKM-1 and MOLM-13 leukemia cell lines. Pharmacol Res Perspect. 2016;4(1):e00206. https://doi.org/10.1002/prp2.206.
11. Ichii M, Oritani K, Murase M, Komatsu K, Yamazaki M, Kyoden R, et al. Molecular targeting of inosine-5′-monophosphate dehydrogenase by FF-10501 promotes erythropoiesis via ROS/MAPK pathway. Leuk Lymphoma. 2018;59(2):448–59. https://doi.org/10.1080/10428194.2017.1339878.
12. Yang H, Fang Z, Wei Y, Bohannan ZS, Ganan-Gomez I, Pierola AA, et al. Preclinical activity of FF-10501-01, a novel inosine-5′-monophosphate dehydrogenase inhibitor, in acute myeloid leukemia. Leuk Res. 2017;59:85–92. https://doi.org/10.1016/j.leukres.2017.05.016.
13. Crowley LC, Marfell BJ, Scott AP, Waterhouse NJ. Quantitation of apoptosis and necrosis by annexin V binding, propidium iodide uptake, and flow cytometry. Cold Spring Harb Protoc. 2016;2016:11. https://doi.org/10.1101/pdb.prot087288.
14. Singh R, Letai A, Sarosiek K. Regulation of apoptosis in health and disease: the balancing act of BCL-2 family proteins. Nat Rev Mol Cell Biol. 2019;20(3):175–93. https://doi.org/10.1038/s41580-018-0089-8.
15. Riedl SJ, Shi Y. Molecular mechanisms of caspase regulation during apoptosis. Nat Rev Mol Cell Biol. 2004;5(11):897–907. https://doi.org/10.1038/nrm1496.
16. Gross A, McDonnell JM, Korsmeyer SJ. BCL-2 family members and the mitochondria in apoptosis. Genes Dev. 1999;13(15):1899–911.
17. Vercammen D, Vandenabeele P, Beyaert R, Declercq W, Fiers W. Tumour necrosis factor-induced necrosis versus anti-Fas-induced apoptosis in L929 cells. Cytokine. 1997;9(11):801–8. https://doi.org/10.1006/cyto.1997.0252.
18. Sano R, Reed JC. ER stress-induced cell death mechanisms. Biochim Biophys Acta. 2013;1833(12):3460–70. https://doi.org/10.1016/j.bbamcr.2013.06.028.
19. Malek K, Boosalis MS, Waraska K, Mitchell BS, Wright DG. Effects of the IMP-dehydrogenase inhibitor, Tiazofurin, in bcr-abl positive acute myelogenous leukemia. Part I. In vivo studies. Leuk Res. 2004;28(11):1125–36. https://doi.org/10.1016/j.leukres.2004.03.003.
20. Kozhevnikova EN, van der Knaap JA, Pindyurin AV, Ozgur Z, van Ijcken WF, Moshkin YM, et al. Metabolic enzyme IMPDH is also a transcription factor regulated by cellular state. Mol Cell. 2012;47(1):133–9. https://doi.org/10.1016/j.molcel.2012.04.030.
21. Kokeny S, Papp J, Weber G, Vaszko T, Carmona-Saez P, Olah E. Ribavirin acts via multiple pathways in inhibition of leukemic cell proliferation. Anticancer Res. 2009;29(6):1971–80.
22. Tzoneva G, Dieck CL, Oshima K, Ambesi-Impiombato A, Sanchez-Martin M, Madubata CJ, et al. Clonal evolution mechanisms in NT5C2 mutant-relapsed acute lymphoblastic leukaemia.

Nature. 2018;553(7689):511–4. https://doi.org/10.1038/nature25186.
23. Ishitsuka K, Hideshima T, Hamasaki M, Raje N, Kumar S, Podar K, et al. Novel inosine monophosphate dehydrogenase inhibitor VX-944 induces apoptosis in multiple myeloma cells primarily via caspase-independent AIF/Endo G pathway. Oncogene. 2005;24(38):5888–96. https://doi.org/10.1038/sj.onc.1208739.
24. Vandenabeele P, Vanden Berghe T, Festjens N. Caspase inhibitors promote alternative cell death pathways. Sci STKE. 2006;2006(358):pe44. https://doi.org/10.1126/stke.3582006pe44.
25. Lin Y, Devin A, Rodriguez Y, Liu ZG. Cleavage of the death domain kinase RIP by caspase-8 prompts TNF-induced apoptosis. Genes Dev. 1999;13(19):2514–26.
26. Chan FK, Shisler J, Bixby JG, Felices M, Zheng L, Appel M, et al. A role for tumor necrosis factor receptor-2 and receptor-interacting protein in programmed necrosis and antiviral responses. J Biol Chem. 2003;278(51):51613–21. https://doi.org/10.1074/jbc.M305633200.
27. Micheau O, Tschopp J. Induction of TNF receptor I-mediated apoptosis via two sequential signaling complexes. Cell. 2003;114(2):181–90.
28. Jonsson CA, Carlsten H. Inosine monophosphate dehydrogenase (IMPDH) inhibition in vitro suppresses lymphocyte proliferation and the production of immunoglobulins, autoantibodies and cytokines in splenocytes from MRLlpr/lpr mice. Clin Exp Immunol. 2001;124(3):486–91.
29. Liao LX, Song XM, Wang LC, Lv HN, Chen JF, Liu D, et al. Highly selective inhibition of IMPDH2 provides the basis of antineuroinflammation therapy. Proc Natl Acad Sci USA. 2017;114(29):E5986–94. https://doi.org/10.1073/pnas.1706778114.
30. Wesselborg S, Engels IH, Rossmann E, Los M, Schulze-Osthoff K. Anticancer drugs induce caspase-8/FLICE activation and apoptosis in the absence of CD95 receptor/ligand interaction. Blood. 1999;93(9):3053–63.
31. Engels IH, Stepczynska A, Stroh C, Lauber K, Berg C, Schwenzer R, et al. Caspase-8/FLICE functions as an executioner caspase in anticancer drug-induced apoptosis. Oncogene. 2000;19(40):4563–73. https://doi.org/10.1038/sj.onc.1203824.
32. Chaigne-Delalande B, Guidicelli G, Couzi L, Merville P, Mahfouf W, Bouchet S, et al. The immunosuppressor mycophenolic acid kills activated lymphocytes by inducing a nonclassical actin-dependent necrotic signal. J Immunol. 2008;181(11):7630–8.
33. Falini B, Nicoletti I, Martelli MF, Mecucci C. Acute myeloid leukemia carrying cytoplasmic/mutated nucleophosmin (NPMc + AML): biologic and clinical features. Blood. 2007;109(3):874–85. https://doi.org/10.1182/blood-2006-07-012252.
34. Leong SM, Tan BX, Bte Ahmad B, Yan T, Chee LY, Ang ST, et al. Mutant nucleophosmin deregulates cell death and myeloid differentiation through excessive caspase-6 and -8 inhibition. Blood. 2010;116(17):3286–96. https://doi.org/10.1182/blood-2009-12-256149.
35. Hanahan D, Weinberg RA. Hallmarks of cancer: the next generation. Cell. 2011;144(5):646–74. https://doi.org/10.1016/j.cell.2011.02.013.
36. Fulda S. Therapeutic exploitation of necroptosis for cancer therapy. Semin Cell Dev Biol. 2014;35:51–6. https://doi.org/10.1016/j.semcdb.2014.07.002.